Microtransfer printing of Al_2O_3-passivated short-wave-infrared PbS quantum dot photoconductors

Nayyera Mahmoud[†‡¶], Willem Walravens[‡¶], Jakob Kuhs[§], Christophe Detavernier[§], Zeger Hens[‡¶], and Gunther Roelkens[†‡]

† Photonics Research Group, Ghent University, Ghent, Belgium

‡ Center for Nano and Biophotonics, Ghent University, Ghent, Belgium

¶ Physics and Chemistry of Nanostructures (PCN), Ghent University, Ghent, Belgium

§ Conformal Coating of Nanomaterials (CoCooN), Ghent University, Ghent, Belgium

Abstract:

Quantum dots (QDs) have attracted considerable attention in the development of various opto-electronic applications. The scalable heterogeneous integration of high quality, yet stable QD films is required for low-cost devices based on these materials. Here, we demonstrate the transfer printing of microscale patterns of Al_2O_3-passivated PbS QD films to realize large-scale integrated photodetector arrays with a 1st excitonic absorption peak at 2.1 μm wavelength. The process provides a facile approach to selectively pick-and-print passivated QDs assemblies on device structures with high precision. Transfer-printed photoconductor devices were realized and characterized at low bias voltage and optical power. Under 10 nW surface normal illumination at 2.1 μm wavelength, the responsivity of our devices obtained at 1 V bias reached a maximum value of 25 A/W and 85 A/W for PbS QD films of 88 nm and 140 nm thick, respectively.

Introduction:

The short-wave infrared (SWIR: 0.9 - 3μm) spectral range enables a wide range of applications, including hyperspectral imaging, sensing based on spectral signatures derived from molecular vibrations, night time surveillance, communications, etc. Detector arrays based on III-V semiconductors, such as InGaAs, are currently driving these applications due to their high quantum efficiency and low dark current at room temperature[2]. Unfortunately, the high material and fabrication cost per unit area prohibit the penetration of the technology into consumer applications. Moreover, monolithic integration on low-cost Si electronics is difficult due to the lattice mismatch between IR materials such as InGaAs and silicon[3], requiring a hybrid integration through flip-chip bonding. Ideally, a good photodetector has to address the challenge of mass fabrication by realizing a relatively cheap material with high photoresponse and ease of integration on commercial silicon read-out integrated circuits.

Colloidal quantum dots (CQDs) are a promising, new material for optical sensing applications due to their unique optical properties. The broad addressable spectrum with a sharp and tunable absorption onset based on size control, the high quantum efficiency and photostability make CQDs a suitable alternative to epitaxially grown semiconductors[4]. Moreover, colloidal synthesis is a low-cost fabrication approach that enables the QD size, shape and surface chemistry to be tuned, thereby optimizing the opto-electronic properties of the QDs for the envisioned application[5,6].

Lead Chalogenides (PbX) nanocrystals (such as PbS CQD) are the most extensively used and commercially available colloidal material for the SWIR region. Various techniques are developed for the integration of CQDs as thin films in electronic and optoelectronic devices. This is conventionally done by techniques that use CQD dispersions, such as drop casting, spin coating, dip coating, Langmuir–Blodgett deposition and doctor blading[7]. Generally, such methods enable low-cost, low temperature and large area formation of QD-based micro- and nanoscale devices.

To realize QD-based devices, post-processing steps to pattern integrated QD films are required. Several patterning processes are reported, each with its advantages and limitations. Micro-scale QD patterns were realized using photolithography either through lift-off[8] or wet etching [9]. High-resolution nanoscale patterning of QD films was realized by electron beam lithography[10]. These methods are limited in usable QD film thickness and surface chemistry and suffer from cross contamination by organic photoresists and chemicals used during etching. Such challenges drive the exploration of new techniques for the scalable integration of uniform, well-defined QD films on a substrate, together with other materials.

Another significant challenge is the deterioration of performance of QD-based devices as a result of irreversible changes of the QDs surface termination, causing a drop in e.g. the photoluminescence quantum yield. This is attributed to the shift of the QD Fermi energy upon oxidation by direct exposure to ambient air. Therefore, to extend the photostability life-time of QDs, encapsulation strategies are required, where organic[11] and inorganic[12] coatings are used. An interesting approach for QD encapsulation is by using atomic layer deposition (ALD), which provides a self-limiting, conformal growth process for surface coatings with nanometer thick films of metal oxides such as Al_2O_3, HfO_2, TiO_2, or ZnO[13]. Thermal ALD grown Al_2O_3 is widely used as an encapsulation layer for the efficient protection of QD-based device stacks against oxidation.

In this paper, we present the first realization of air-stable SWIR PbS photoconductor arrays through micro-transfer printing. Micron-sized Al_2O_3 passivated PbS QD (Al_2O_3/PbS QD) patterns are selectively transferred onto arrays of planar interdigitated (Ti/Au) electrodes on a thermally oxidized silicon substrate, mimicking an underlying electronic read-out circuit using a structured poly-dimethyl-siloxane (PDMS) stamp. We demonstrate a protocol for a facile

solvent-free transfer of multiple high-quality passivated QD patches to the target substrate per single print. The transfer is done from a densely populated QD/Si source substrate, allowing maximum usage of the deposited QD films to print on multiple substrates. The to-be-transferred QD film area is defined by patterning the Al_2O_3. Only patterning the Al_2O_3 is sufficient to peel-off the QD film underneath the Al_2O_3 during the transfer printing process. This introduces an efficient way for wafer-scale integration of QD patches / devices on either electronic or photonic circuits, or any other substrate. The fabrication process of Al_2O_3/PbS QD films on the source substrate and the transfer printing process flow are reported. Finally, current-voltage measurements in dark and under low optical intensities at 2.1 μm wavelength are carried out to evaluate the performance of the realized devices.

Results and Discussion

Transfer printing process flow:

The transfer printing is realized by a commercial micro-transfer printer (X-Celeprint, model μTP-100 model). The printing process involves using a patterned PDMS stamp installed on a glass holder to pick up the material from the source substrate placed onto the source chuck. Then the stamp moves to the target chuck and prints with a sub-micrometer accuracy on a predefined position on the target substrate. After completion, the stamp moves and presses down on a cleaning pad to remove residual print material (if necessary)[14]. In our presented work, arrays of Al_2O_3/PbS QD patches (realized on the source substrate) are printed on pre-fabricated interdigitated contact electrodes on the target substrate. In this process, a 100 μm × 800 μm patterned PDMS post is used to pick up and print the desired material. Picking and printing is realized by controlling the adhesion of the QD patch to the stamp [15,16]. The position of the QD patches on the source substrate as well as the position of the devices on the target wafer are pre-defined to allow a fully automated transfer printing operation. The alignment of the stamp with source and target substrate is monitored by a camera mounted on top of the transparent stamp and stamp holder. A schematic illustration of the transfer-printing process flow is shown in **Figure (1)**.

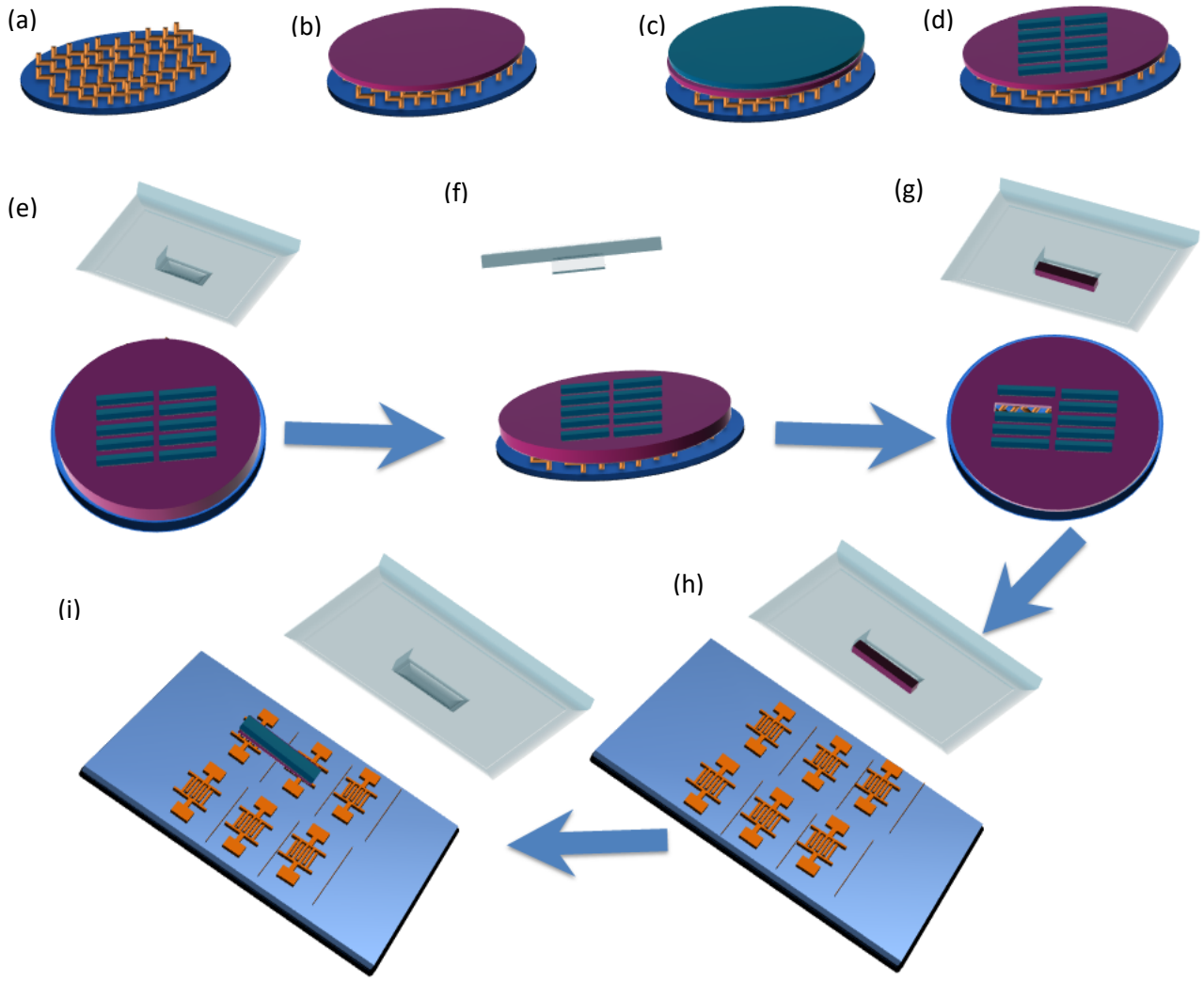

Figure 1 Schematic illustration of solvent-free Al_2O_3/PbS QD film transfer printing. (a-d) Schematic illustration of source substrate preparation, which starts with surface modification by ODTS-SAM, QD film spin coating with layer-by-layer ligand exchange and finally deposition and patterning of ALD-Al_2O_3. (e-i) Schematic illustration of the transfer of Al_2O_3/PbS patches and their printing on multiple interdigitated electrodes realized on an oxidized silicon wafer resulting in the formation of a series of photoconductors per single transfer printing operation.

Preparation of source substrates starts with using PbS QDs (11.8 nm) synthesized by adapting the method introduced by Jonathan S. Owen[17]. According to the absorbance spectrum shown in **Figure (2a)**, the obtained PbS QDs exhibit a 1st excitonic transition at λ=2.1 μm. The quality and particle size distribution was confirmed by TEM shown in **Figure (2a-inset)**.

Silicon (Si) substrates are firstly modified with self-assembled octadecyltrichlorosilane (ODTS) monolayers to facilitate delamination during the transfer printing process. The highly ordered alkyl

chains of ODTS substantially diminish the surface energy without introducing surface roughness (only ~0.2 nm) and shows a good adherence to the primary QD layer, resulting in a uniform QD film[18,19]. CQD film deposition is made by means of a layer-by-layer spin coating on the ODTS-Si substrates. For each coated layer, the native oleic acid ligands were removed upon exposure to a (1M) n-butylamine in methanol (MeOH) solution. These deposition cycles were repeated until the desired film thickness was reached. The ligand exchange was confirmed using Fourier transform infrared spectroscopy (FTIR). **Figure (2b)** illustrates the FTIR spectra of a QD film before and after exposure to the n-butylamine solution. The signatures of the COO^- and C-H vibrations in the range of 1300-1500cm^{-1} and 2800-3000cm^{-1} respectively, indicate the presence of oleate ligands at the QD surface[20,21]. The substantial reduction of the intensity of these features confirms the ligands removal. The resultant dry QD film is then passivated through a thermal ALD deposition of Al_2O_3 to form typically 70 nm thick layer[22]. Finally, A dense array of Al_2O_3 patterns on top of the PbS QD films is realized through photolithography and subsequent wet etching. It is worth noting that during the transfer-printing process, the passivated QD patches were still covered by this photoresist layer (~3.5µm thick) to prevent the brittle patches from being damaged during printing on the target substrate.

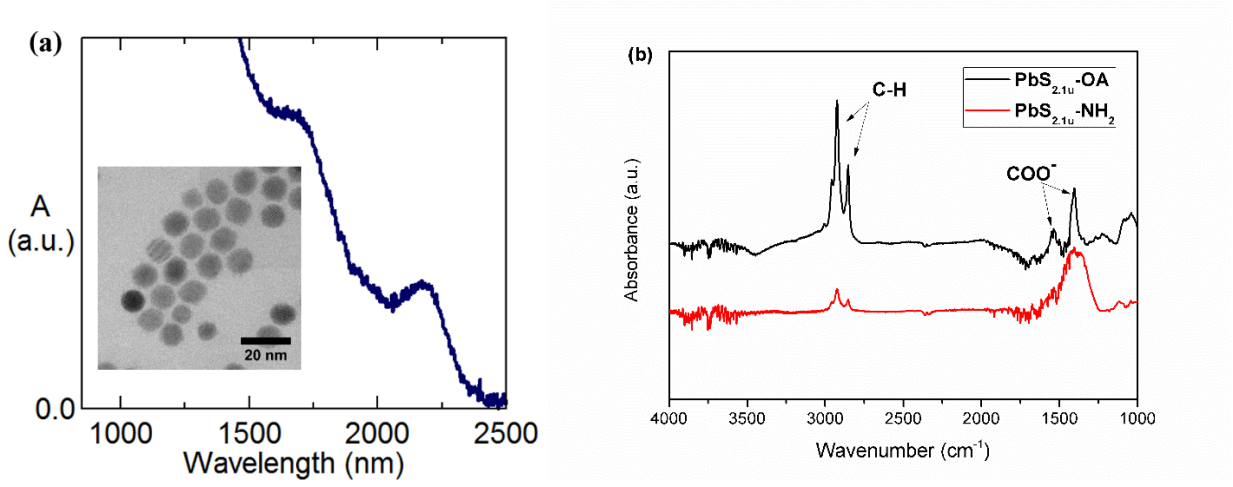

Figure 2. (a)Absorption spectrum of OA-terminated colloidal PbS QDs. (b) FTIR specta of oleate capped PbS QD film (black) and butylamine capped PbS QDs (red). Inset of (a) Transmission electron micrograph of oleate capped PbS QDs

For target substrates, planarized arrays of interdigitated Ti/Au contacts were defined through optical lithography, e-beam metal deposition and lift-off on a thermally oxidized silicon wafer.

Before metal deposition, the SiO_2 is partially etched through reactive ion etching (RIE) with the same pattern as the interdigitated finger electrides such that after metal pattern definition planar substrates were achieved with a surface topography of 5nm.

The strong interactions between the QD surface and the Al_2O_3 film compared to their weak interactions to the ODTS-Si substrate allow excellent kinetic control of the QD patterning/pickup from the source without the need to exert a high stamp pressure and a slow retraction of the stamp to peel-off the pattern. All previous work[23–25] on QD transfer printing reported that the pick-up of bare QD films from source substrates was achieved at a slow peeling rate (typically 1 $mm.s^{-1}$). However, in our work, we report a significant improvement that is attributed to the presence of the Al_2O_3 passivation layer, forming an 'exo-skeleton' for the QD film and providing a much faster and high-quality pickup. This leads to the conclusion that the Al_2O_3 layer not only stabilizes the QDs against oxidation, but also facilitates QD film patterning and improves the pick-up yield and printing throughput.

Figure 3.a shows an optical image of a well-defined vacant area on the source substrate after pick-up of an Al_2O_3/QD patch, while the bare QD film still is present around the peeled area. **Figure 3.b** shows an SEM image after printing of this patch on three-in-a-row interdigitated Ti/Au electrodes (after removal of the protective photoresist on top of the quantum dot patch using acetone). As discussed above, the Ti/Au electrodes were planarized to enable a smooth transfer of the QD material. A cross section (**Figure 3.c)** of the transfer-printed patterns validate a good contact with the Au electrodes.

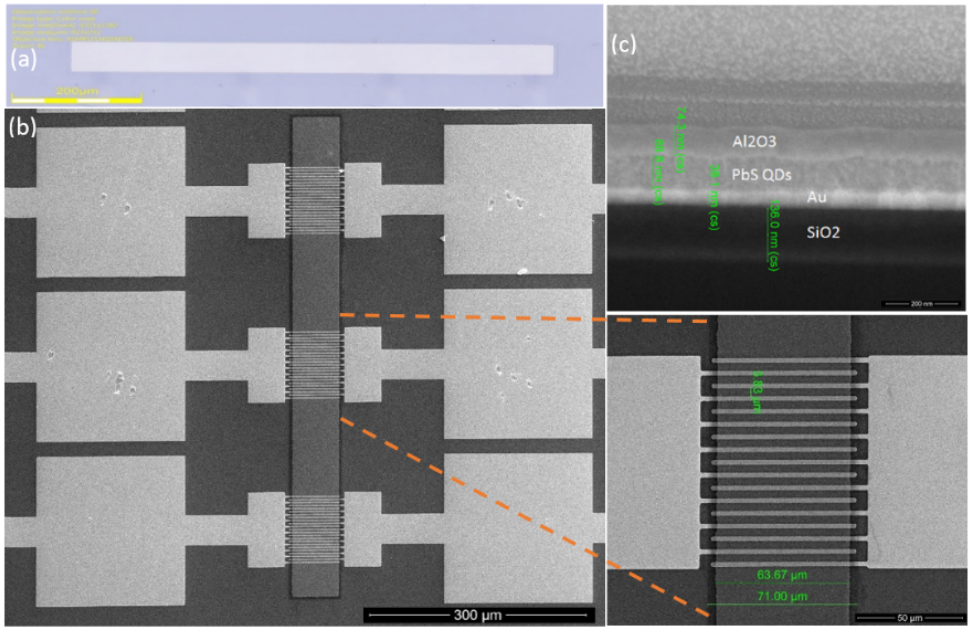

Figure 3 (a) optical image of the source substrate after pattern pick-up, (b) transfer-printed Al_2O_3/PbS QD film, (c) cross section on a pair of interdigitated Au contacts.

The patches were printed by peeling the stamp at a relatively slow peeling rate to allow the release (0.2 mm/s). **Figure 4** shows an optical microscope image of multiple Al_2O_3/PbS QDs patches of different lengths and widths printed with high yield. This demonstrates the excellent scalability of printing high quality passivated QDs with high precision (+/- 1.5 µm 3σ alignment accuracy).

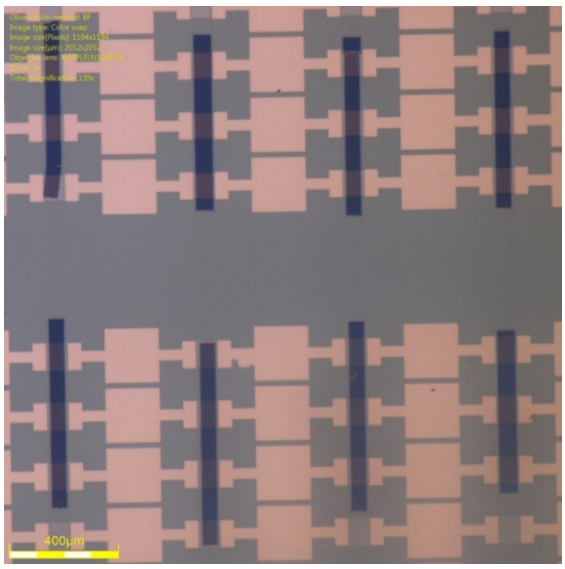

Figure 4 Optical image of multiple arrays of printed Al_2O_3/PbS QD patches on interdigitated electrodes

The impact of the QD film thickness on the micro-transfer-printing yield was evaluated by transfer printing QD films of 88, 110 and 140 nm thickness, all capped with 70 nm Al_2O_3. In all three cases arrays of QD films were 100% successfully defined, picked-up and printed on target devices with high precision.

Al_2O_3/PbS QD photoconductor characterization:

Two different photoconductor structures with QD film thickness of 88 nm and 140 nm were characterized. The fabricated devices are 80 × 80 μm^2 in area, with interdigitated metal fingers of 80 μm long, 2 μm wide and on a pitch of 4 μm. Each device is provided with two contact pads of 100 ×100 μm^2. **Figure 5(a)** displays typical current-voltage curves of a printed Al_2O_3/PbS QDs device with a 140 nm QD film thickness in the dark and under illumination at 2.1 μm wavelength. The linear behavior of the dark/photo-current indicates excellent ohmic contacts, which reflects the high quality of the printed Al_2O_3/PbS patches. The dark resistance (R_d) is about 65 kΩ, which drops by more than 50% (30 kΩ) under 140 μW optical illumination. The responsivity (R) as a function of applied voltage is calculated from the net photocurrent, based on the equation (1):

$$\boldsymbol{R = \frac{I_{light} - I_{Dark}}{P_{in}}} \quad (1)$$

, where I_{light} is the total current under illumination, I_{dark} is the dark current and P_{in} is the optical input power. The responsivity shows a linear behavior with the applied bias voltage as shown in **figure 5(b)**

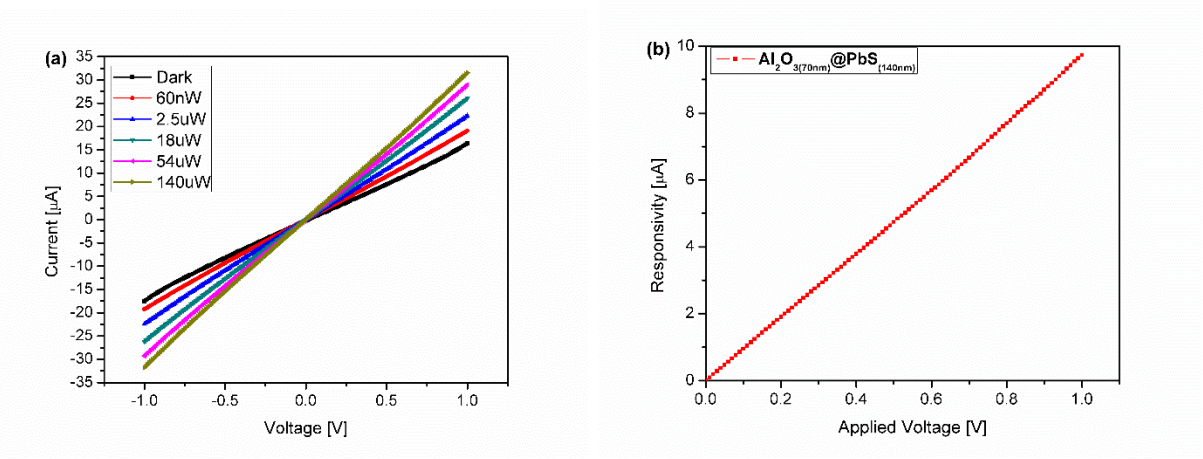

Figure 5(a) Current-voltage characteristics for surface illumination at 2.1 μm wavelength. (b) Responsivity versus bias voltage for 1uW optical input power

The detector responsivity was investigated at low bias voltage (1V) to evaluate their potential integration to CMOS read-out circuits. **Figures 6(a) and 6(b)** show the two detectors' responsivity as a function of incident input power. The responsivity shows a strong power dependence reaching a maximum value of about 85 A/W and 25 A/W at 10 nW illumination for 88 nm and 140 nm thick PbS QD devices, respectively. Upon illumination, a primary photocurrent arises by photon absorption causing the creation and separation of an electron-hole pair. The large responsivity is attributed to the characteristic high gain of photoconductors due to the long lifetime of the photogenerated carriers with respect to transit time. At low illumination levels, all photogenerated carriers are captured by the QD surface traps, producing a longer lifetime and therefore a higher responsivity. Alternatively, at higher illumination levels, the photogenerated carrier density is expected to exceed the capacity of trap states, thereby diminishing the photoresponse.

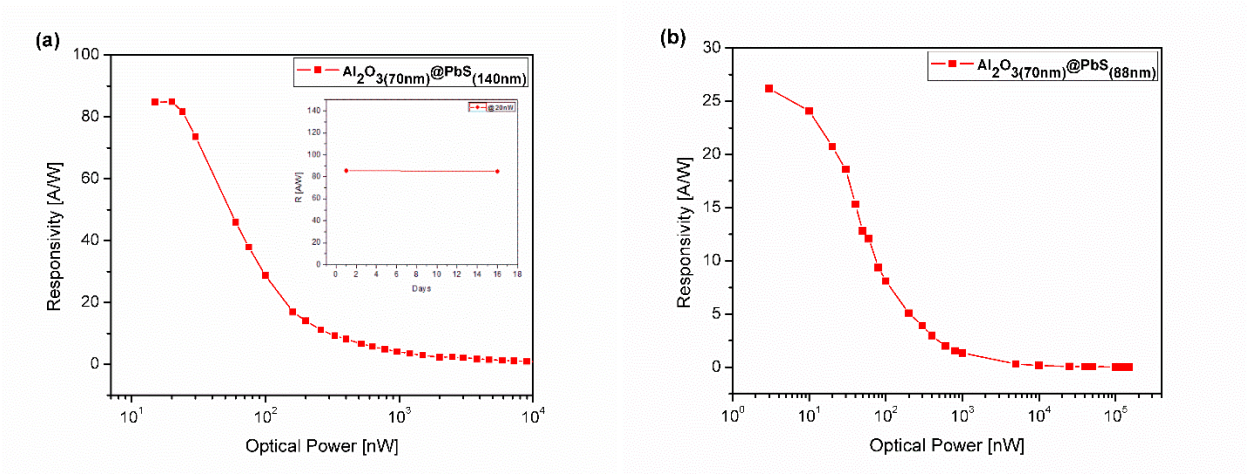

Figure 6 (a) Responsivity versus optical power of Al_2O_3 (70nm)/PbS(140nm) and (b) Al_2O_3 (70nm)/PbS (88nm) photoconductors, respectively. Responsivity is measured at 1 V applied voltage for optical input powers ranging from 10 nW to 140µW. Inset of (a) shows responsivity as a function of time (> 2 weeks time frame) under 20nW illumination.

Covering the QD films by Al_2O_3 during transfer-printing proved to be effective to avoid degradation with time at ambient conditions,. The passivated devices showed no degradation and explicit photostability for 16 days, at least, **figure 6 (a-inset)**. Longer lifetime tests are currently ongoing.

Conclusion:

We report the micro-transfer-printing of Al_2O_3/PbS photoconductors on interdigitated electrode structures. Our approach allows the efficient integration of well-defined, air-stable and high-quality QD films. The Al_2O_3 cap plays an important role in QDs pattern definition, facile transfer-printing and passivation. The pick-up and printing was optimized to reach close to 100% yield. Photoconductors developed using this approach exhibit high responsivity at 2.1µm with maximum values of 25 A/W and 85 A/W for QD films of thickness 88 nm and 140 nm, respectively, at 1 V bias. This transfer printing approach enables the intimate integration of QD films / photoconductors with different cut-off wavelengths, enabling advanced, low-cost devices such as SWIR hyperspectral imagers.

Method:

1.1 Synthesis of PbS QDs: In a three-neck flask, 0.939 g of Pb-oleate and 10 mL of n-dodecane were mixed and heated to 150 ºC. Into this solution was injected 1.25 mL of a 0.16 M solution of N-hexyl-N'-dodecylthiourea in diglyme. Five minutes later, a second injection of 0.75 mL of a 0.8 M solution of N-hexyl-N'-dodecylthiourea in diglyme was injected. After a total reaction time of 20 minutes, the reaction was quenched and the QDs precipitated by injecting 10 mL of methyl acetate. After separation by centrifugation, the resulting black pellet was purified further by washing 4 additional times with toluene and methyl acetate as solvent and antisolvent respectively. Synthesis of N-hexyl-N'-dodecylthiourea was done by a stirring solution of 6.47 g of dodecylamine (34.9 mmole, 1 eq.) in 20 mL of toluene, 5.0 g of hexyl isothiocyanate (34.9 mmole, 1 eq.) was added. After letting the mixture cool down to room temperature, the white precipitate was dried in vacuum for 24 hours.

1.2 Source substrate preparation:

1.2.1 Silicon Cleaning: Si substrates were cleaned by first rinsing with acetone, isopropylalcohol (IPA) and deionized (DI) water, followed by a 30 min O_2 plasma treatment. The samples were then treated by 10% HF solution for 5 min to remove the native silicon oxide. Next, a Piranha treatment (H_2SO_4:H_2O_2 of ratio 2:1) was applied at 80ºC for 20 min to facilitate the salinization step. Finally, the substrates were rinsed with water, dried with N_2 and stored in a glove box for further use.

1.2.2 Synthesis of ODTS-Si: A self-assembled monolayer (SAM) of silane was covalently bonded to Si through a chemical reaction of the hydrogen-terminated Si surface with a 10mM solution of octadecyltrichlorosilane in anhydrous hexane for 2 hours under N_2 condition. The substrates were then baked for 20 min at 120 ºC to ensure covalent crosslinking on the entire surface. Eventually, the substrates were cleaned by ultrasonication with chloroform and DI water to eliminate extra-unbonded alkylsilanes.

1.2.3 PbS QD deposition: Films were completely prepared under N_2 in a glove box. The film deposition was done through a layer-by-layer spin coating of a solution of 20mg/ml OA-PbS QDs (in heptane) at 2000 rpm for 15s. OA-PbS QDs were then decapped by dipping the substrate for 1 min in 1M n.butylamine in methanol solution, followed by rinsing in pure methanol to reveal the surface of the nanoparticles by removing extra n.butylamine. The resulting layer was dried by N_2 before the deposition was repeated in order to obtain the desired QD film thickness. A thickness of around 88 nm and 140nm was achieved by 5 and 8 coating cycles, respectively.

1.2.4 Al_2O_3 ALD Process: A thermal ALD process was carried out, using trimethylaluminum (TMA) and H_2O as precursors. The deposition temperature was 100 ºC. The samples were exposed to 5s of TMA and 5s of water vapor at a pressure $5x10^4$ Pa. 1000 ALD cycles resulted in a 70 nm thick Al_2O_3 film. The thickness was monitored by X-Ray Reflectometry (XRR).

1.2.5 Micro-patterning of Al_2O_3: Standard photolithography was done, where AZ5214E positive resist was spin coated on the samples and baked at 120ºC for 3 min. The substrates were exposed through a contact photomask using a SUSS MA6 mask aligner and then were developed in AZ400 developer. Subsequently, a diluted KOH solution of pH 12 was used to etch the exposed parts of the Al_2O_3 layer.

1.3 Target substrate preparation: A series of patterned metal contacts were fabricated on a thermally oxidized silicon wafer. The oxide thickness was 300nm. Planarized interdigitated Ti/Au contacts were fabricated by a combination of RIE dry etching of the SiO_2, E-beam Ti/Au metal deposition in the formed trenches and subsequent lift-off. The metal fingers are 80 μm long, 2 μm wide and have a pitch of 4 μm. Each device is provided with two contact pads of area 100×100 μm^2.

1.4 Transfer printing: Transfer printing was carried out using an X-Celeprint micro-TP100 lab-scale printer. A patterned viscoelastic PDMS stamp - with a post of 100 µm × 800 µm- was laminated against donor substrates, then quickly peeled back to lift the as-fabricated Al_2O_3 pattern along with the underlying PbS QD film, thereby transferring the structure to the PDMS stamp. The patterns were covered with resist during the transfer printing operation in order to prevent cracking of the film by the pressure applied during printing. The pick-up velocity and pressure applied were optimized to reach a pick-up yield of 100%. Printing the patterns was accomplished by laminating the stamp against the target substrate and peeling back at a slow rate (0.2 mm s^{-1}) for a clean, crack-free release. Finally, the substrates were washed in acetone and IPA to remove photoresist.

1.5 Electrical Measurements: Current-voltage measurements were taken in ambient conditions, using a Keithley measure unit. Photocurrent under different illumination intensities was measured by surface illumination of the photoconductors with a fiber-coupled laser at 2.1 µm wavelength. The bias was swept between -1 and +1 V with a step of 10 mV.

Acknowledgment: We acknowledge support by the European Commission via the Marie-Sklodowska Curie action Phonsi (H2020-MSCA-ITN-642656).

References:

(2) Hansen, M. P.; Malchow, D. S. Overview of SWIR Detectors, Cameras, and Applications; Vavilov, V. P., Burleigh, D. D., Eds.; International Society for Optics and Photonics, 2008; Vol. 6939, p 69390I.

(3) Svensson, J.; Dey, A. W.; Jacobsson, D.; Wernersson, L.-E. III–V Nanowire Complementary Metal–Oxide Semiconductor Transistors Monolithically Integrated on Si. *Nano Lett.* **2015**, *15* (12), 7898–7904.

(4) Moreels, I.; Lambert, K.; Smeets, D.; De Muynck, D.; Nollet, T.; Martins, J. C.; Vanhaecke, F.; Vantomme, A.; Delerue, C.; Allan, G.; et al. Size-Dependent Optical Properties of Colloidal PbS Quantum Dots. *ACS Nano* **2009**, *3* (10), 3023–3030.

(5) Kovalenko, M. V.; Manna, L.; Cabot, A.; Hens, Z.; Talapin, D. V.; Kagan, C. R.; Klimov, V. I.; Rogach, A. L.; Reiss, P.; Milliron, D. J.; et al. Prospects of Nanoscience with Nanocrystals. *ACS Nano* **2015**, *9* (2), 1012–1057.

(6) Kagan, C. R.; Lifshitz, E.; Sargent, E. H.; Talapin, D. V. Building Devices from Colloidal Quantum Dots. *Science* **2016**, *353* (6302), aac5523.

(7) Crisp, R. W.; Kroupa, D. M.; Marshall, A. R.; Miller, E. M.; Zhang, J.; Beard, M. C.; Luther, J. M. Metal Halide Solid-State Surface Treatment for High Efficiency PbS and PbSe QD Solar Cells. *Sci. Rep.* **2015**, *5* (1), 9945.

(8) Lambert, K.; Moreels, I.; Thourhout, D. Van; Hens, Z. Quantum Dot Micropatterning on Si. *Langmuir* **2008**, *24* (11), 5961–5966.

(9) Hu, C.; Aubert, T.; Justo, Y.; Flamee, S.; Cirillo, M.; Gassenq, A.; Drobchak, O.; Beunis, F.; Roelkens, G.; Hens, Z. The Micropatterning of Layers of Colloidal Quantum Dots with Inorganic Ligands Using Selective Wet Etching. *Nanotechnology* **2014**, *25* (17), 175302.

(10) Nandwana, V.; Subramani, C.; Yeh, Y.-C.; Yang, B.; Dickert, S.; Barnes, M. D.; Tuominen, M. T.; Rotello, V. M. Direct Patterning of Quantum Dot Nanostructures via Electron Beam Lithography. *J. Mater. Chem.* **2011**, *21* (42), 16859.

(11) Jagtap, A.; Goubet, N.; Livache, C.; Chu, A.; Martinez, B.; Gréboval, C.; Qu, J.; Dandeu, E.; Becerra, L.; Witkowski, N.; et al. Short Wave Infrared Devices Based on HgTe Nanocrystals with Air Stable Performances. *J. Phys. Chem. C* **2018**, *122* (26), 14979–14985.

(12) Devloo-Casier, K.; Geiregat, P.; Ludwig, K. F.; van Stiphout, K.; Vantomme, A.; Hens, Z.; Detavernier, C.; Dendooven, J. A Case Study of ALD Encapsulation of Quantum Dots: Embedding Supported CdSe/CdS/ZnS Quantum Dots in a ZnO Matrix. *J. Phys. Chem. C* **2016**, *120* (32), 18039–18045.

(13) Puurunen, R. L. Surface Chemistry of Atomic Layer Deposition: A Case Study for the Trimethylaluminum/Water Process. *J. Appl. Phys.* **2005**, *97* (12), 121301.

(14) Carlson, A.; Bowen, A. M.; Huang, Y.; Nuzzo, R. G.; Rogers, J. A. Transfer Printing Techniques for Materials Assembly and Micro/Nanodevice Fabrication. *Adv. Mater.* **2012**, *24* (39), 5284–5318.

(15) De Groote, A.; Cardile, P.; Subramanian, A. Z.; Fecioru, A. M.; Bower, C.; Delbeke, D.; Baets, R.; Roelkens, unther; Roelkens, G.; Abbasi, A.; et al. Transfer-Printing-Based Integration of Single-Mode Waveguide-Coupled III-V-on-Silicon Broadband Light Emitters " III-V-on-Silicon Photonic Devices for Optical Communication and Sensing " A Printable Form of Silicon for High Performance Thin Film. *Laser Photon. Rev. Appl. Phys. Lett* **2015**, *2* (84), 969–1004.

(16) Meitl, M. A.; Zhu, Z.-T.; Kumar, V.; Lee, K. J.; Feng, X.; Huang, Y. Y.; Adesida, I.; Nuzzo, R. G.; Rogers, J. A. Transfer Printing by Kinetic Control of Adhesion to an Elastomeric Stamp. *Nat. Mater.* **2006**, *5* (1), 33–38.

(17) Hendricks, M. P.; Campos, M. P.; Cleveland, G. T.; Jen-La Plante, I.; Owen, J. S. A Tunable Library of Substituted Thiourea Precursors to Metal Sulfide Nanocrystals. *Science* **2015**, *348* (6240), 1226–1230.

(18) Hsu, H.-W.; Chang, W.-C.; Tung, S.-H.; Liu, C.-L. Surface Energy-Mediated Self-Patterning for High Performance Spray-Deposited Organic Field Effect Transistors. *Adv. Mater. Interfaces* **2016**, *3* (11), 1500714.

(19) Kim, D. H.; Lee, H. S.; Yang, H.; Yang, L.; Cho, K. Tunable Crystal Nanostructures of Pentacene Thin Films on Gate Dielectrics Possessing Surface-Order Control. *Adv. Funct. Mater.* **2008**, *18* (9), 1363–1370.

(20) Konstantatos, G.; Sargent, E. H. Solution-Processed Quantum Dot Photodetectors. *Proc. IEEE* **2009**, *97* (10), 1666–1683.

(21) Zhang, D.; Song, J.; Zhang, J.; Wang, Y.; Zhang, S.; Miao, X. A Facile and Rapid Synthesis of Lead Sulfide Colloidal Quantum Dots Using in Situ Generated H2S as the Sulfur Source. *CrystEngComm* **2013**, *15* (13), 2532.

(22) Hu, C.; Gassenq, A.; Justo, Y.; Devloo-Casier, K.; Chen, H.; Detavernier, C.; Hens, Z.; Roelkens, G. Air-Stable Short-Wave Infrared PbS Colloidal Quantum Dot Photoconductors Passivated with Al_2O_3 Atomic Layer Deposition. *Appl. Phys. Lett.* **2014**, *105* (17), 171110.

(23) Kim, T.-H.; Cho, K.-S.; Lee, E. K.; Lee, S. J.; Chae, J.; Kim, J. W.; Kim, D. H.; Kwon, J.-Y.; Amaratunga, G.; Lee, S. Y.; et al. Full-Colour Quantum Dot Displays Fabricated by Transfer Printing. *Nat. Photonics* **2011**, *5* (3), 176–182.

(24) Kim, T.-H.; Chung, D.-Y.; Ku, J.; Song, I.; Sul, S.; Kim, D.-H.; Cho, K.-S.; Choi, B. L.; Min Kim, J.; Hwang, S.; et al. Heterogeneous Stacking of Nanodot Monolayers by Dry Pick-and-Place Transfer and Its Applications in Quantum Dot Light-Emitting Diodes. *Nat. Commun.* **2013**, *4*, 2637.

(25) Kim, B. H.; Nam, S.; Oh, N.; Cho, S.-Y.; Yu, K. J.; Lee, C. H.; Zhang, J.; Deshpande, K.; Trefonas, P.; Kim, J.-H.; et al. Multilayer Transfer Printing for Pixelated, Multicolor Quantum Dot Light-Emitting Diodes. *ACS Nano* **2016**, *10* (5), 4920–4925.